

Antioxidant enzyme inhibitors enhance singlet oxygen-induced cell death in HL-60 cells

SUN YEE KIM, SU MIN LEE & JEEN-WOO PARK

School of Life Sciences and Biotechnology, College of Natural Sciences, Kyungpook National University, Taegu 702-701, South Korea

Accepted by Professor N. Taniguchi

(Received 22 April 2006; in revised form 7 June 2006)

Abstract

Singlet oxygen is a highly reactive form of molecular oxygen that may harm living systems by oxidizing critical cellular macromolecules and it also promotes deleterious processes such as cell death. The protective role of antioxidant enzymes against singlet oxygen-induced oxidative damage in HL-60 cells was investigated in control and cells pre-treated with diethyldithiocarbamic acid, aminotriazole and oxalomalate, specific inhibitors of superoxide dismutase, catalase and NADP⁺-dependent isocitrate dehydrogenase, respectively. Upon exposure to rose bengal (20 μM)/light (15 min), which generates singlet oxygen, to HL-60 cells, the viability was lower and the lipid peroxidation and oxidative DNA damage were higher in inhibitor-treated cells as compared to control cells. We also observed the significant increase in the endogenous production of reactive oxygen species as well as the significant decrease in the intracellular GSH level in inhibitor-treated HL-60 cells exposed to singlet oxygen. Upon exposure to rose bengal (3 μM)/light (15 min), which induced apoptotic cell death, a clear inverse relationship was observed between the control and inhibitor-treated HL-60 cells in their susceptibility to apoptosis. These results suggest that antioxidant enzymes play an important role in cellular defense against singlet oxygen-induced cell death including necrosis and apoptosis.

Keywords: Singlet oxygen, antioxidant enzymes, necrosis, apoptosis, redox status

Introduction

Singlet molecular oxygen (¹O₂), an electronically excited state of oxygen which results from the promotion of an electron to high energy orbitals, is produced in mammalian cells under normal and pathophysiological conditions [1]. The photodynamic action of some drugs and pigments is also mediated through singlet oxygen [2]. ¹O₂ is a highly reactive form of molecular oxygen that may harm living systems by oxidizing critical cellular macromolecules, including lipids, nucleic acids and proteins, and it also promotes deleterious processes such as lipid peroxidation, membrane damage and cell death [3].

Biological systems have evolved an effective and complicated network of defense mechanisms which

enable cells to cope with lethal oxidative environments. These defense mechanisms involve antioxidant enzymes, such as superoxide dismutase (SOD), which catalyze the dismutation of O₂⁻ to H₂O₂ and O₂ [4], catalase and peroxidases which remove hydrogen peroxide and hydroperoxides [5]. The isocitrate dehydrogenases (EC1.1.1.41 and EC1.1.1.42) catalyze oxidative decarboxylation of isocitrate to α-ketoglutarate and require either NAD⁺ or NADP⁺, producing NADH and NADPH, respectively. NADPH is an essential reducing equivalent for the regeneration of reduced glutathione (GSH) by glutathione reductase and for the activity of NADPH-dependent thioredoxin system [6], both are important in the protection of cells from oxidative

Correspondence: J.-W. Park, School of Life Sciences and Biotechnology, College of Natural Sciences, Kyungpook National University, Taegu 702-701, South Korea. Fax: 82 53 943 2762. E-mail: parkjw@knu.ac.kr

damage. Therefore, NADP⁺-dependent isocitrate dehydrogenase (ICDH) may play an antioxidant role during oxidative stress. As reactive oxygen species (ROS) appear to be mediators of the cell death including necrosis and apoptosis, enzymes that regulate the fate of such species may be of great importance in the regulation of cells against oxidative stress-induced cell death.

In the present study the role of antioxidant enzymes in cellular defense against the singlet oxygen-induced oxidative damage was investigated using the control HL-60 cells and HL-60 cells treated with diethyldithiocarbamic acid (DETC), aminotriazole (ATZ), or oxalomalate. DETC and ATZ have been known as specific inhibitors of SOD and catalase, respectively [3]. Oxalomalate, a tricarboxylic acid (α -hydroxy- β -oxalosuccinic acid) formed in *in vitro* and *in vivo* by condensation of oxaloacetate and glyoxylate, has been known to be a potent competitive inhibitor of ICDH [7]. The results revealed that inhibitors of antioxidant enzymes exacerbate singlet oxygen-induced oxidative damage in HL-60 cells subsequently induce necrosis and apoptosis depending on the dose of singlet oxygen.

Materials and methods

Materials

RPMI 1640, fetal bovine serum (FBS), penicillin-streptomycin were obtained from GIBCO-BRL (Rockville, MD). Rose bengal, oxalomalate, DETC, ATZ, *tert*-butylhydroperoxide (*t*-BOOH), pyrogallol, β -NADP⁺, GSSG, GSH, glucose-6-phosphate, 3-(4,5-dimethylthiazol-2-yl)-2,5-diphenyltetrazolium bromide (MTT), avidin-tetramethylrhodamine isothiocyanate (TRITC), anti-rabbit IgG TRITC conjugated secondary antibody, anti-rabbit IgG fluorescein isothiocyanate (FITC) conjugated secondary antibody, propidium iodide (PI), 4',6-diamidino-2-phenylindole (DAPI), and glutathione reductase were obtained from Sigma Chemical Co. (St Louis, MO). Anti-human dinitrophenyl (DNP) antibody was obtained from Calbiochem (La Jolla, CA). 2',7'-Dichlorofluorescein diacetate (DCFH-DA), *t*-butoxycarbonyl-Leu-Met-7-amino-4-chloromethylcoumarin (CMAC), and diphenyl-1-pyrenylphosphine (DPPP) were purchased from Molecular Probes (Eugene, OR). Antibodies against Bcl-2, lamin B, cleaved caspase-3, and cleaved poly(ADP-ribose) polymerase (PARP) were purchased from Santa Cruz (Santa Cruz, CA).

Cell culture and cytotoxicity assay

Human promyelocytic leukemia cell line HL-60 (American Type Culture Collection, Rockville, MD,

USA) was grown in RPMI 1640 culture medium supplemented with 10% (v/v) FBS, penicillin (50 units/ml), and 50 μ g/ml streptomycin at 37°C in a 5% CO₂ – 95% air humidified incubator. Cells treated with various concentrations of RB were irradiated with white light from a 100 W tungsten bulb at 30 cm from the petri dish and cell viability was assessed by MTT assay. Cell viability is expressed as a percentage of the absorbance seen in the untreated control cells.

Enzyme assay

Cells were collected at 10,000g for 10 min at 4°C and were washed once with cold PBS. Briefly, cells were homogenized with a Dounce homogenizer in sucrose buffer (0.32 M sucrose, 10 mM Tris-Cl, pH 7.4). Cell homogenates were centrifuged at 1000g for 5 min, and the supernatants were further centrifuged at 15,000g. The resulting supernatants were used as the cytosolic fractions. Protein concentration was determined by the method of Bradford using the reagents purchased from Bio-Rad. The supernatants were added by 1/10 volume of 10X PBS containing 1% Triton-X100, which finally made the solution 1X PBS containing 0.1% Triton-X100. The supernatants were used to measure the activities of several cytosolic enzymes. The activity of ICDH was measured by the production of NADPH at 340 nm [8]. The reaction mixture for ICDH activity contained 50 mM MOPS, pH 7.2, 5 mM threo-DS-isocitrate, 35.5 mM triethanolamine, 2 mM NADP⁺, 1 mM ADP, 2 mM MgCl₂, and 1 μ g/ml rotenone. One unit of ICDH activity is defined as the amount of enzyme catalyzing the production of 1 μ mol of NADPH/min. Catalase activity was measured with the decomposition of hydrogen peroxide, which was determined by the decrease in absorbance at 240 nm. SOD activity in cell extracts was assayed spectrophotometrically using a pyrogallol assay, where one unit of activity is defined as the quantity of enzyme which reduces the superoxide-dependent color change by 50%. Glucose 6-phosphate dehydrogenase activity was measured by following the rate of NADP⁺ reduction at 340 nm using the procedure described [8]. Glutathione peroxidase activity in the crude extracts was measured by the standard indirect method based on NADPH oxidation by *t*-BOOH in the presence of excess glutathione and glutathione reductase, as previously described [9]. For colorimetric assay for caspase activity, cells were collected with a cell scraper, washed with PBS, mixed with lysis buffer (50 mM HEPES, pH 7.4, 100 mM NaCl, 0.1% CHAPS, 1 mM DTT, and 0.1 mM EDTA) for 10 min at 0°C, and centrifuged at 10,000g for 10 min at 4°C. Supernatant containing 100 μ g protein was added to reaction buffer (100 mM HEPES, pH 7.4, 0.5 mM PMSF, 10 mM dithiothreitol, 1 mM EDTA, and 10% glycerol) containing Ac-DEVD-pNA (Calbiochem,

San Diego, CA, USA) and incubated for 2 h at 37°C. The absorbance was then monitored at 405 nm to determine the caspase activity.

FACS

To determine the portion of apoptotic cells, cells were analyzed with PI staining [10]. HL-60 cells were collected at 2000g for 5 min and washed once with cold PBS, fixed in 70% ethanol, decant ethanol by centrifuge and stained with 1 ml of solution containing 50 mg/ml PI, 1 mg/ml RNase A, 1.5% Triton X-100 for at least 1 h in the dark at 4°C. Labeled nuclei were subjected to flow cytometric analysis and then gated on light scatter to remove debris, and the percentage of nuclei with a sub-G₁ content was considered apoptotic cells.

Cellular redox status

The concentration of total glutathione was determined by the rate of formation of 5-thio-2-nitrobenzoic acid at 412 nm ($\epsilon = 1.36 \times 10^4 \text{ M}^{-1} \text{ cm}^{-1}$) as described by Akerboom and Sies [11], and GSSG was measured by the DTNB-GSSG reductase recycling assay after treating GSH with 2-vinylpyridine [12]. The intracellular GSH level was also determined by using a GSH-sensitive fluorescence dye CMAC. HL-60 cells (1×10^6 cells/ml) were incubated with 5 μM CMAC cell tracker for 30 min. The images of CMAC cell tracker fluorescence by GSH was analyzed by the Zeiss Axiovert 200 inverted microscope at fluorescence 4,6-diamidino-2-phenylindole (DAPI) region (excitation, 351 nm; emission, 380 nm) [13]. Intracellular ROS production was measured using the oxidant-sensitive fluorescent probe DCFH-DA with confocal microscopy [9]. Intracellular hydrogen peroxide concentrations were determined using a ferric sensitive dye, xylenol orange, as described [14].

Cellular oxidative damage

Lipid peroxidation was estimated by using a fluorescent probe DPPP as described by Okimoto et al. [15]. After HL-60 cells were incubated with 5 μM DPPP for 15 min in the dark, cells were exposed to RB (20 μM)/light (15 min). The images of DPPP fluorescence by reactive species were analyzed by the Zeiss Axiovert 200 inverted microscope at fluorescence DAPI region (excitation, 351 nm; emission, 380 nm). 8-OH-dG levels of HL-60 cells were estimated by using a fluorescent binding assay as described by Struthers et al. [16]. After HL-60 cells were exposed to RB/light, cells were fixed and permeabilized with ice-cold methanol for 15 min. DNA damage was visualized with avidin-conjugated TRITC (1: 200 in PBS for 1 h) for fluorescent microscope with 488 nm excitation and 580 nm emission.

Immunoblot analysis

Proteins were separated on 10% SDS-polyacrylamide gel, transferred to nitrocellulose membranes, and subsequently subjected to immunoblot analysis using appropriate antibodies. Immunoreactive antigen was then recognized by using horseradish peroxidase-labeled anti-rabbit IgG and an enhanced chemiluminescence detection kit (Amersham Pharmacia Biotech).

Quantitation of relative fluorescence

The averages of fluorescence intensity from fluorescence images were calculated as described [17].

Replicates

Unless otherwise indicated, each result described in this paper is representative of at least three separate experiments.

Results

Measurement of SOD, catalase and ICDH activities revealed that HL-60 cells pre-treated with 1 mM DETC, 20 mM ATZ and 3 mM oxalomalate for 2 h, respectively, contained significantly reduced activity of target enzymes compared to that of the untreated control (Figure 1). Because cellular antioxidants act in a concerted manner as a team, it is important to investigate whether the modulation in cellular antioxidant enzyme activity caused concomitant alterations in the activity of other major antioxidant enzymes. Therefore, we measured the activities of

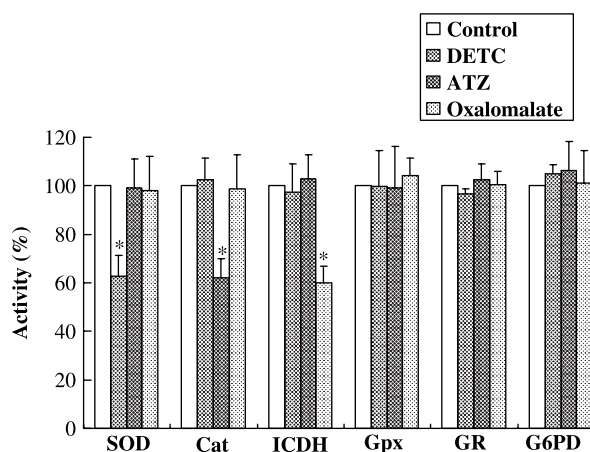


Figure 1. Activity of antioxidant enzymes in HL-60 cells untreated and treated with inhibitors. Activity of untreated cells is expressed as 100%. Results shown are the mean \pm SD of five independent experiments. SOD, superoxide dismutase; Cat, catalase; ICDH, NADP⁺-dependent isocitrate dehydrogenase; Gpx, glutathione peroxidase; GR, Glutathione reductase; G6PD, glucose 6-phosphate dehydrogenase. * $P < 0.01$ compared to untreated control.

the following enzymes: SOD, catalase, ICDH, glutathione reductase, glutathione peroxidase, and glucose 6-phosphate dehydrogenase. As shown in Figure 1, the activities of these major antioxidant enzymes were similar to control and inhibitor-treated cells examined except the target enzyme for specific inhibitor, suggesting that reduction of one antioxidant enzyme activity did not affect the activities for these other antioxidant enzymes.

To study the effect of SOD, catalase, and ICDH on the relationship between singlet oxygen and cytotoxicity, control HL-60 cells and HL-60 cells pre-treated with specific inhibitors were exposed to different doses of photoactivated rose bengal, the singlet oxygen generator. As shown in Figure 2, control cells were significantly more resistant to singlet oxygen than oxalomalate-treated cells. Control cells showed a survival of 80% after exposure to RB (20 μ M)/light (15 min) whereas inhibitor-treated cells showed a survival of \sim 50%. The cells exhibiting the lower SOD, catalase, or ICDH activity were killed to a greater extent upon exposure to RB/light, indicating that these enzymes may be involved in protecting cells from damage induced by singlet oxygen.

GSH is one of the most abundant intracellular antioxidants and determination of changes in its concentration provides an alternative method of monitoring oxidative stress within cells. It has been shown that GSH sensitive fluorescent dye CMAC can be employed as a useful probe to evaluate the level of intracellular GSH [13]. Cellular GSH levels in inhibitor-treated HL-60 cells exposed to RB/light were significantly decreased (Figure 3(A)). These results strongly suggest that diminished antioxidant enzyme activity by specific inhibitors resulted in the perturbation of cellular antioxidant mechanisms by

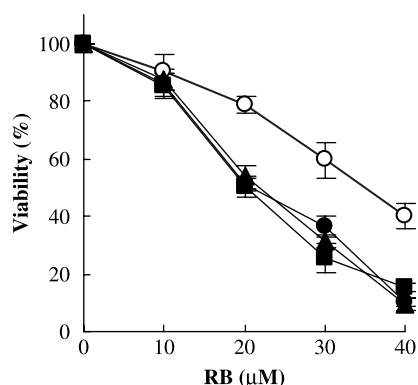


Figure 2. Effect of antioxidant enzyme inhibitors on the viability of HL-60 cells upon exposure to RB/light. Control (open circles), DETC (closed circles), ATZ (closed rectangles), and oxalomalate-treated (closed triangles) HL-60 cells were exposed to various concentrations of RB for 15 min with illumination, and viability of cells was determined by using a MTT assay. Survival of untreated cells was expressed as 100%. Results shown are the mean \pm SD of five independent experiments.

the depletion of GSH presumably through the decrease in NADPH generation. One important parameter of GSH metabolism is the ratio of GSSG/total GSH (GSH_t) which may reflect the efficiency of GSH turnover. When the cells were exposed to RB/light, the ratio of cellular $[GSSG]/[GSH_t]$ was significantly higher in inhibitor-treated cells than in control cells (Figure 3(B)). This data indicates that GSSG in inhibitor-treated cells was not reduced as efficiently as in control cells. To investigate whether or not the difference in viability of the HL-60 cells upon exposure to RB/light is associated with ROS formation, the levels of intracellular peroxides in HL-60 cells were measured by confocal microscopy with the oxidant-sensitive probe DCFH-DA. As shown in Figure 3(C), DCF fluorescence intensity was significantly increased in cells treated with inhibitors as compared to that of the control upon exposure to RB/light. The data strengthen the conclusion that decreased activity of antioxidant enzymes provides the cytotoxic action by increasing the steady-state level of intracellular oxidants upon exposure to RB/light. The pre-treatment of inhibitors also resulted in a significantly higher intracellular level of H_2O_2 as compared to that of untreated control with the exposure of RB/light (Figure 3(D)).

As indicative markers of oxidative damage to cells, the occurrence of oxidative DNA damage and lipid peroxidation were evaluated. Recently, it has been shown that DPPP is a suitable fluorescence probe to monitor lipid peroxidation within cell membrane specifically. DPPP reacts with lipid hydroperoxides stoichiometrically to give highly fluorescent product DPPP oxide [15]. When exposed to RB (20 μ M)/light (15 min), DPPP fluorescent intensity was increased markedly in HL-60 cells pre-treated with inhibitors as compared to the untreated control (Figure 4(A)). The reaction of intracellular ROS with DNA resulted in numerous forms of base damage, and 8-OH-dG is one of the most abundant and most studied lesions generated. Because 8-OH-dG causes misreplication of DNA [18], it has been implicated as a possible cause of mutation and cancer. Therefore, 8-OH-dG has been used as an indicator of oxidative DNA damage *in vivo* and *in vitro* [19]. Recently, it has been shown that 8-OH-dG level is specifically measured by a fluorescent binding assay using avidin-conjugated TRITC [16]. The fluorescent intensity which reflects the endogenous levels of 8-OH-dG in DNA was significantly increased when inhibitor-treated HL-60 cells were exposed to RB (20 μ M)/light (15 min) (Figure 4(B)).

The exposure of HL-60 cells to RB (3 μ M)/light (15 min), which resulted in the shift of redox status to a pro-oxidative state to a lesser extent compared to that of RB (20 μ M)/light (15 min), caused shrinkage of the cell and the plasma membrane blebbing under

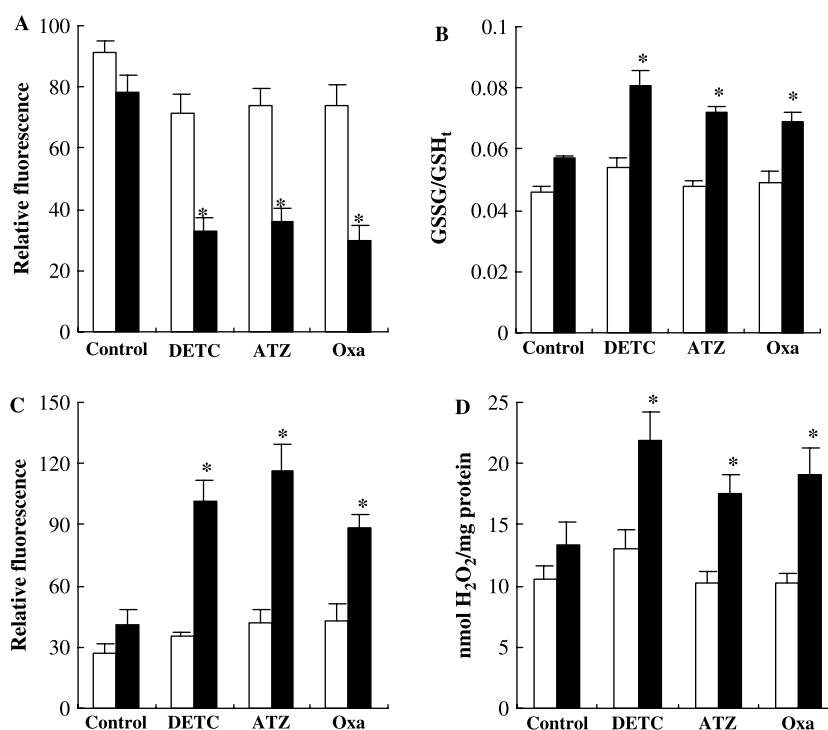


Figure 3. Effect of antioxidant enzyme inhibitors on the cellular redox status of HL-60 cells exposed to RB/light. Control and inhibitor-treated HL-60 cells were exposed to 20 μ M RB for 15 min with illumination. (A) Effect of antioxidant enzyme inhibitors on GSH levels. Fluorescence image of CMAC-loaded cells was obtained under microscopy. The averages of fluorescence intensity were calculated as described [17]. (B) Ratios of GSSG vs total GSH pool. (C) Fluorescence image of DCFH-DA loaded cells was obtained under laser confocal microscopy. The relative intensity of DCF fluorescence was calculated as described [17]. (D) Production of hydrogen peroxide in HL-60 cells was determined by the method described under Material and Methods. Results shown are the mean \pm SD of five independent experiments. Open and shaded bars represent HL-60 cells unexposed and exposed to RB, respectively. * $P < 0.01$ compared to unexposed inhibitor-treated cells.

light microscopy (data not shown). Figure 5 shows a typical cell cycle plot of HL-60 cells that were untreated or treated with RB (3 μ M)/light (15 min). Apoptotic cells were estimated by calculating the number of subdiploid cells in the cell cycle histogram. When cells were exposed to RB/light, apoptotic cells were increased markedly in inhibitor-treated cells as compared to control cells.

We evaluated changes in the apoptotic marker proteins as a result of treatment with RB (3 μ M)/light (15 min) and the influence of inhibitors of antioxidant enzymes on these proteins. Caspase-3 activation in HL-60 cells was assessed by caspase colorimetric assay and by immunoblot analysis of lysates from cells that had been exposed to RB/light. Caspase-3 activity increased significantly higher in inhibitor-treated cells than control cells upon exposure to RB/light (Figure 6(A)). As shown in Figure 6(B), RB (3 μ M)/light (15 min) induced cleavage of caspase-3, however, the cleavage was significantly higher in inhibitor-treated cells. Induction of the formation of fragments which represents proteolytic cleavage of PARP and lamin B, indicates an oncoming apoptotic process. The cleaved products of PARP and lamin B increased markedly in inhibitor-treated cells compared to control cells upon exposure to RB/light.

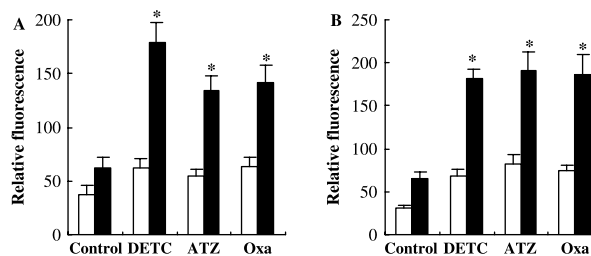


Figure 4. Effect of antioxidant enzyme inhibitors on cell damage of HL-60 cells exposed to RB/light. Control and inhibitor-treated HL-60 cells were exposed to 20 μ M RB for 15 min with illumination. (A) Visualization of lipid peroxidation in HL-60 cells. Cells (1×10^6 cells/ml) were stained with 5 μ M DPPH for 15 min. Fluorescence images were obtained under microscopy. The relative intensity of fluorescence was calculated as described [17]. (B) 8-OH-dG levels in HL-60 cells. Cells were fixed and permeabilized immediately after exposure to RB/light. 8-OH-dG levels reflected by the binding of avidin-TRITC were visualized by a fluorescence microscope with 488 nm excitation and 580 nm emission. The relative intensity of fluorescence was calculated as described [17]. Results shown are the mean \pm SD of five independent experiments. Open and shaded bars represent HL-60 cells unexposed and exposed to RB, respectively. * $P < 0.01$ compared to unexposed inhibitor-treated cells.

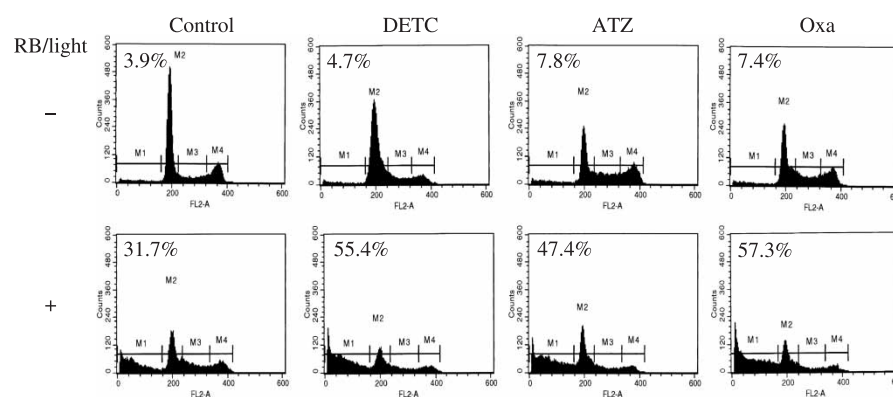


Figure 5. Singlet oxygen-induced apoptosis in inhibitor-treated HL-60 cells. Control and inhibitor-treated HL-60 cells were exposed to 3 μ M RB for 15 min with illumination. Cell cycle analysis with cellular DNA content was examined by flow cytometry. The sub-G₁ region (presented as "M1") includes cells undergoing apoptosis. The number of each panel refers to the percentage of apoptotic cells.

Taken together, singlet oxygen-induced cleavage of procaspase-3 into the active form of caspase-3 and caspase-3 induces degradation of PARP or lamin B. The results also indicate that inhibitors exhibit an enhanced effect on the singlet oxygen-induced apoptosis. The role of mitochondrial pathway of apoptosis in the singlet oxygen-induced death of HL-60 cells were examined by immunoblot analysis of the abundance of Bcl-2, an antiapoptotic protein. As shown in Figure 6(B), the abundance of Bcl-2 in HL-60 cells was significantly decreased in inhibitor-treated cells as compared to that of control cells when exposed to RB (3 μ M)/light (15 min).

Discussion

It is well established that $^1\text{O}_2$ can be generated in cells such as under conditions of oxidative stress [20], from decomposition of lipid peroxides or by spontaneous

dismutation of superoxide [3,21]. In addition, both naturally occurring compounds such as riboflavin [22] and many xenobiotics, such as psoralene [23], porphyrins [24] and tetracyclins [25] can generate $^1\text{O}_2$ inside cells when irradiated by visible light. Singlet oxygen is most often generated *in vitro* by photosensitization reactions. Irradiation of the sensitizer dye, such as RB, mediates photoreactions through an excited triplet state which acts either by hydrogen atom or electron transfer reactions (type I) or by transferring the excited energy, forming singlet oxygen, which then reacts with the target molecules (type II) [3]. Light induced a few diseases including erythropoietic protoporphyria, pellagra and cataractogenesis have been attributed in part to the toxicity of $^1\text{O}_2$ [26,27]. On the other hand, it has been suggested that singlet oxygen is the primary active species in a novel cancer treatment modality known as photodynamic therapy [28].

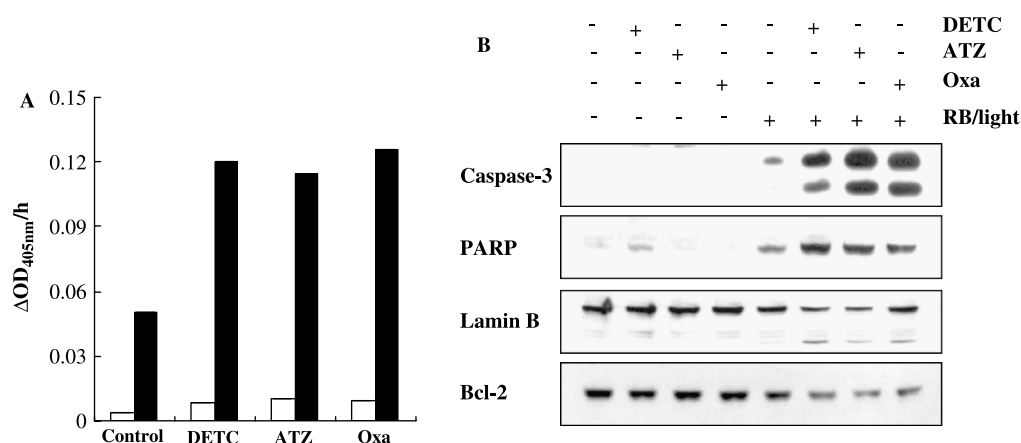


Figure 6. Singlet oxygen-induced modulation of apoptotic marker proteins in inhibitor-treated HL-60 cells. (A) HL-60 cells exposed to 3 μ M RB for 3 min with illumination were lysed and centrifuged. The supernatant was then added to Ac-DEVD-pNA and subjected to caspase colorimetric activity. Protease activity of caspase-3 was calculated by monitoring the absorbance at 405 nm. Open and shaded bars represent HL-60 cells unexposed and exposed to RB/light, respectively. (B) HL-60 cells were exposed to 3 μ M RB for 15 min with illumination. Cell extracts (20 μ g protein) were subjected to 10–12.5% SDS-PAGE and immunoblotted with antibodies against cleaved caspase-3, cleaved PARP, lamin B, and Bcl-2.

When cells are grown in air, NADPH must be used to maintain a level of GSH as well as reduced thioredoxin to combat oxidative damage. Glutathione reductase converts GSSG to GSH in the cell using NADPH as a reductant [29]. The oxidized form of thioredoxin, with a disulfide bridge between the half-cystines, is reduced by NADPH in the presence of a flavoprotein, thioredoxin reductase [30]. Reduced thioredoxin may provide reducing equivalents to several enzymes including thioredoxin peroxidases and methionine sulfoxide reductase, presumably involving the defense against oxidative stress. The pentose phosphate pathway is considered to be a major source of cellular reducing power, with glucose-6-phosphate dehydrogenase catalyzing the key NADPH-producing step. It is well documented that this pathway, specifically glucose-6-phosphate dehydrogenase, plays a protective role during oxidative stress [31,32]. However, it is possible that other enzymes which generate NADPH may have roles in oxidative stress resistance. ICDH in the cytosol of rat liver has been proven to have an approximately 20 times higher specific activity than glucose-6-phosphate dehydrogenase [33]. We reported that the control of cellular redox balance and oxidative damage is one of the primary functions of ICDH in cytosol of NIH3T3 cells [8].

To demonstrate the singlet oxygen-induced intracellular oxidation, we evaluated intracellular oxidants after exposure to RB/light. We noted that RB/light caused an increase in intracellular oxidants such as hydroperoxides in HL-60 cells. However, the increase in hydroperoxides was significantly higher in inhibitor-treated cells than in control cells. These data suggest that the enzymatic action of antioxidant enzymes protects cells from the cytotoxic actions of singlet oxygen by decreasing the steady-state level of intracellular oxidants. Intracellular oxidants may induce the damage to protein, DNA, and lipids, which results in cellular damage. Cells have the lower activity of antioxidant enzymes show a significant increase in oxidative damage to lipid and DNA, emphasizing the essential protective role of antioxidant enzymes in mitigating such damage.

GSH is a well-known antioxidant which is usually present as the most abundant low-molecular-mass thiol in most organisms. It has various functions in the defense against oxidative stress and xenobiotic toxicity [34]. It can act as the electron donor for glutathione peroxidase in animal cells, and also directly reacts with ROS. GSH is readily oxidized to glutathione disulfide (GSSG) by the glutathione peroxidase reaction, as well as the reaction with ROS which may subsequently cause the reduction of GSH level. In the meantime, antioxidant enzymes act as a team. The inactivation of one antioxidant enzyme may affect the cellular antioxidant defense system including the glutathione redox status under oxidative stress. In our study,

exposure of RB/light to inhibitor-treated cells directly affected the glutathione redox status reflected by the total GSH level and the ratio of [GSSG]/[GSH_T] and the intracellular ROS in the same condition. These results indicate that singlet oxygen modulates the cellular redox balance presumably by depleting GSH. Consequently, the perturbation of the balance between oxidants and antioxidants leads to a pro-oxidant condition.

At the lower concentrations of photoactivated RB, such as 3 μM RB, apoptotic cell death was induced in HL-60 cells, and the susceptibility to apoptosis was significantly increased in inhibitor-treated cells when compared to that of control cells. Cleavage of caspase-3 and its target proteins such as PARP and lamin B, a signature event of apoptosis, was induced by RB/light. Inhibitors of antioxidant enzymes enhanced programmed cell death by increasing apoptotic features including caspase activation and decreasing anti-apoptotic molecules (Bcl-2), presumably via perturbation of redox status.

The results of this study demonstrate distinct differences between cells exhibit the lower activity of antioxidant enzymes and control cells in regard to the number of surviving cells and the accumulation of peroxides, lipid peroxidation products and 8-OH-dG in DNA upon exposure to higher concentration of singlet oxygen as well as the susceptibility to apoptosis at the lower concentration of singlet oxygen. These results suggest that SOD, catalase and ICDH protect cells against singlet oxygen-induced oxidative stress and subsequent cell death.

Acknowledgements

This work was supported by grants from the Korea Research Foundation (KRF-2005-070-C00100) and the basic science program of the Ministry of Commerce, Industry and Energy (R12-2003-002-04002-0).

References

- [1] Kanofsky JR. Singlet oxygen production by biological systems. *Chem Biol Interact* 1989;70:1–28.
- [2] Weishaupt KR, Gomer CJ, Dougherty TJ. Identification of singlet oxygen as the cytotoxic agent in photoinactivation of a murine tumor. *Cancer Res* 1976;36:2326–2329.
- [3] Halliwell B, Gutteridge JMC. *Free radicals in biology and medicine*. Oxford: Oxford Press; 1999.
- [4] McCord JM, Fridovich I. Superoxide dismutase. An enzymic function for erythrocuprein (hemocuprein). *J Biol Chem* 1969;244:6049–6055.
- [5] Chance B, Sies H, Boveris A. Hydroperoxide metabolism in mammalian organs. *Physiol Rev* 1979;59:527–605.
- [6] Fridovich I. Superoxide radical: An endogenous toxicant. *Annu Rev Pharmacol Toxicol* 1983;23:239–257.
- [7] Ingebretsen OC. Mechanism of the inhibitory effect of glyoxylate plus oxaloacetate and oxalomalate on the

- NADP-specific isocitrate dehydrogenase. *Biochim Biophys Acta* 1976;452:302–309.
- [8] Lee SM, Koh HJ, Park DC, Song BJ, Huh TL, Park JW. Cytosolic NADP⁺-dependent isocitrate dehydrogenase status modulates oxidative damage to cells. *Free Radic Biol Med* 2002;32:1185–1196.
- [9] Krall J, Speranza MJ, Lynch RE. Paraquat-resistant HeLa cells: Increased cellular content of glutathione peroxidase. *Arch Biochem Biophys* 1991;286:311–315.
- [10] Darzynkiewicz Z, Sharpless T, Staiano-Coico L, Melamed MR. Sub-compartments of the G₁ phase of cell cycle detected by flow cytometry. *Proc Natl Acad Sci USA* 1980;77:6696–6699.
- [11] Akerboom TPM, Sies H. Assay of glutathione, glutathione disulfide, and glutathione mixed disulfides in biological samples. *Methods Enzymol* 1981;77:373–382.
- [12] Anderson ME. Determination of glutathione and glutathione disulfide in biological samples. *Methods Enzymol* 1985;113:548–555.
- [13] Tauskela JS, Hewitt K, Kang LP, Comas T, Gendron T, Hakim A, Hogan M, Durkin J, Morley P. Evaluation of glutathione-sensitive fluorescent dyes in cortical culture. *Glia* 2001;30:329–341.
- [14] Jiang ZY, Hunt JV, Wolff SP. Ferrous ion oxidation in the presence of xylenol orange for detection of lipid hydroperoxide in low density lipoprotein. *Anal Biochem* 1992;202:384–389.
- [15] Okimoto Y, Watanabe A, Niki E, Yamashita T, Noguchi N. A novel fluorescent probe diphenyl-1-pyrenylphosphine to follow lipid peroxidation in cell membranes. *FEBS Lett* 2000;474:137–140.
- [16] Struthers L, Patel R, Clark J, Thomas S. Direct detection of 8-oxodeoxyguanosine and 8-oxoguanine by avidin and its analogues. *Anal Biochem* 1998;255:20–31.
- [17] Sundaresan M, Yu ZX, Ferrans CJ, Irani K, Finkel T. Requirement for generation of H₂O₂ for platelet-derived growth factor signal transduction. *Science* 1995;270:296–299.
- [18] Shibutani S, Takeshita M, Grollman AP. Insertion of specific base during DNA synthesis past the oxidation-damaged base 8-oxodG. *Nature* 1991;349:431–434.
- [19] Park JW, Floyd RA. Lipid peroxidation products mediate the formation of 8-hydroxydeoxyguanosine in DNA. *Free Radic Biol Med* 1992;12:245–250.
- [20] Sies H. Biochemistry of oxidative stress. *Angew Chem Int Ed Engl* 1986;25:1058–1072.
- [21] Krinsky NI. Membrane photochemistry and photobiology. *Photochem Photobiol* 1974;20:532–535.
- [22] Joshi PC. Comparison of the DNA-damaging property of photosensitized riboflavin via singlet oxygen (¹O₂) and superoxide radical O₂^{•-} mechanisms. *Toxicol Lett* 1985;26:211–217.
- [23] de Mol NG, van Henegouven GMJB, van Beele B. Singlet oxygen formation by sensitization of furocoumarins complexed with, or bound covalently to DNA. *Photochem Photobiol* 1981;34:661–666.
- [24] Weishaupt KR, Gomer CJ, Dougherty TJ. Identification of singlet oxygen as the cytotoxic agent in photoinactivation of a murine tumor. *Cancer Res* 1976;36:2326–2329.
- [25] Hasan T, Khan AU. Phototoxicity of the tetracyclines: Photosensitized emission of singlet delta dioxygen. *Proc Natl Acad Sci USA* 1986;83:4604–4606.
- [26] Mathews-Roth MM. Beta-carotene therapy for erythropoietic protoporphyria and other photosensitivity diseases. *Biochimie* 1986;68:875–884.
- [27] Egorov SI, Babizhaev MA, Krasnovskii AA, Shredova AA. Photosensitized generation of singlet molecular oxygen by endogenous substances of the eye lens. *Biofizika* 1987;32:169–171.
- [28] Henderson BW, Dougherty TJ. How does photodynamic therapy work? *Photochem Photobiol* 1992;55:145–157.
- [29] Pigeolet E, Corbisier P, Houbion A, Lambert D, Michiels C, Raes M, Zachary MD, Remacle J. Glutathione peroxidase, superoxide dismutase, and catalase inactivation by peroxides and oxygen derived free radicals. *Mech Ageing* 1990;51:283–297.
- [30] Holmgren A. Thioredoxin. *Annu Rev Biochem* 1985;54:237–271.
- [31] Kletzien RK, Harris PKW, Foellmi LA. Glucose-6-phosphate dehydrogenase: A “housekeeping” enzyme subject to tissue-specific regulation by hormones, nutrients, and oxidant stress. *FASEB J* 1994;8:174–181.
- [32] Pandolfi PP, Sonati F, Rivi R, Mason P, Grosveld F, Luzzatto L. Targeted disruption of the housekeeping gene encoding glucose 6-phosphate dehydrogenase (G6PD): G6PD is dispensable for pentose synthesis but essential for defense against oxidative stress. *EMBO J* 1995;14:5209–5215.
- [33] Veech RL, Eggleston LV, Krebs HA. The redox state of free nicotinamide-adenine dinucleotide phosphate in the cytoplasm of rat liver. *Biochem J* 1969;115:609–619.
- [34] Meister A, Anderson ME. Glutathione. *Annu Rev Biochem* 1983;52:711–760.